

Elementary excitations of Heisenberg ferrimagnetic spin chains

Shoji Yamamoto

Department of Physics, Faculty of Science, Okayama University, Tsushima, Okayama 700, Japan

S. Brehmer and H.-J. Mikeska

Institut für Theoretische Physik, Universität Hannover, 30167 Hannover, Germany

(Received 30 October 1997)

We numerically investigate elementary excitations of the Heisenberg alternating-spin chains with two kinds of spins, 1 and 1/2, antiferromagnetically coupled to each other. Employing a recently developed efficient Monte Carlo technique as well as an exact-diagonalization method, we verify the spin-wave argument that the model exhibits two distinct excitations from the ground state which are gapless and gapped. The gapless branch shows a quadratic dispersion in the small-momentum region, which is of the ferromagnetic type. With the intention of elucidating the physical mechanism of both excitations, we make a perturbation approach from the decoupled-dimer limit. The gapless branch is directly related to spin 1's, while the gapped branch originates from cooperation of the two kinds of spins.

[S0163-1829(98)00921-7]

I. INTRODUCTION

Extensive efforts have so far been devoted to verifying Haldane's conjecture¹ that the one-dimensional spin- S Heisenberg antiferromagnet exhibits qualitatively different properties according to whether S is integer or half odd integer. The nontrivial energy gap immediately above the ground state was precisely estimated using a number of numerical tools not only in the spin-1 case²⁻⁴ but also in the spin-2 case,^{5,6} while the valence-bond-solid model⁷ introduced by Affleck *et al.* significantly contributed to the understanding of the physical mechanism of the so-called Haldane massive phase. On the other hand, developing the $O(3)$ nonlinear- σ -model quantum field theory,¹ Affleck⁸ pointed out that even integer-spin chains should be critical if a certain interaction is added to the pure Heisenberg Hamiltonian. Actually various numerical methods⁹⁻¹⁵ revealed that the spin quantum number is no longer the criterion for the critical behavior in a wider Hamiltonian space. Recently several authors^{16,17} even suggested the appearance of the Haldane-gap phases in half-odd-integer-spin chains with a magnetic field applied. Thus the low-temperature properties of one-dimensional quantum antiferromagnets with one kind of spin have more and more been elucidated.

In such circumstances, there has appeared brand-new attempts¹⁸⁻³⁰ to explore the quantum behavior of mixed-spin chains with two kinds of spins. These studies are further classified according to their main interests. Several authors¹⁸⁻²¹ have been devoting their efforts to finding quantum integrable Hamiltonians and clarifying their critical behavior. Although the models considered are generally complicated, the generic description of a certain family of Hamiltonians is interesting in itself and even allows us to guess the essential consequences of mixed-spin chains. A distinct attention is directed to mixed-spin chains with the simplest interaction between the two kinds of spins. Alternating-spin Heisenberg antiferromagnets with a singlet ground state^{26,29} again present us the nontrivial gap

problem.^{1,8} Recently Fukui and Kawakami²⁶ have made a nonlinear- σ -model approach for a few models of this kind and have discussed a generic criterion for the critical mixed-spin chains. Their finding may stimulate many theoreticians to numerically investigate a variety of mixed-spin Hamiltonians and even lead to synthesis of novel mixed-spin-chain materials. On the other hand, considering that all the mixed-spin-chain compounds synthesized so far exhibit a finite ground-state magnetization,³¹ we take a great interest in alternating-spin Heisenberg antiferromagnets with ferrimagnetic ground states. This is the subject we discuss in the present article.

Let us introduce a Hamiltonian of alternatively aligned two kinds of spins S and s which are antiferromagnetically coupled to each other:

$$\mathcal{H} = J \sum_{j=1}^N (S_j \cdot s_j + \delta s_j \cdot S_{j+1}), \quad (1.1)$$

where $S_j^2 = S(S+1)$, $s_j^2 = s(s+1)$, and N is the number of unit cells. The bond alternation δ has been introduced for a discussion presented afterwards. We assume $S > s$ in the following without losing generality. Because of the noncompensating sublattice magnetizations, this system exhibits the ferrimagnetism instead of the antiferromagnetism. Applying the Lieb-Mattis theorem³² to the Hamiltonian (1.1), we immediately find $(S-s)$ N -fold degenerate ground states. The Goldstone theorem³³ further allows us to expect a gapless excitation from the ferrimagnetic ground state. Therefore we here take little interest in the simple problem whether the system is gapped or gapless. Alcaraz and Malvezzi²² investigated the two cases of $(S,s)=(1,1/2)$ and $(S,s)=(3/2,1/2)$ and actually showed that in both cases the chain is described in terms of the $c=1$ Gaussian conformal field theory under the existence of exchange anisotropy. Suggesting that this should be the generic scenario for arbitrary ferrimagnetic Heisenberg chains, they further predicted the appearance of quadratic dispersion relations at the Heisenberg

points, which means that the model possesses a ferromagnetic character. On the other hand, applying the spin-wave theory to the model, two groups^{24,25} have recently predicted that there exists a gapped branch of elementary excitations as well as a gapless ferromagnetic branch. Their prediction is quite interesting because it implies the coexistence of the ferromagnetism and the antiferromagnetism in the ferrimagnets. This is the motivation for the present study. Employing a quantum Monte Carlo technique and an exact-diagonalization method, we here calculate energy eigenvalues of the elementary excitations with the total magnetization $\sum_{j=1}^N (S_j^z + s_j^z) \equiv M = (S-s)N \mp 1$, which correspond to the ferromagnetic and the antiferromagnetic branches, respectively. The numerical results are compared not only with the spin-wave calculation but also with a perturbation approach from the decoupled-dimer limit ($\delta=0$).

II. THE SPIN-WAVE APPROACH

First, we briefly review the spin-wave-theory result,^{24,25} which allows us to have a qualitative view of the low-energy structure. We start from a Néel state with $M=(S-s)N$, namely, we define the bosonic operators for the spin deviation in each sublattice as

$$\begin{aligned} S_j^+ &= \sqrt{2S}a_j, & S_j^- &= \sqrt{2S}a_j^\dagger, & S_j^z &= S - a_j^\dagger a_j, \\ s_j^+ &= \sqrt{2s}b_j^\dagger, & s_j^- &= \sqrt{2s}b_j, & s_j^z &= -s + b_j^\dagger b_j. \end{aligned} \quad (2.1)$$

In order to obtain the dispersion relations of the spin-wave excitations, we handle the boson Hamiltonian up to quadratic order. We define the momentum representation of the bosonic operators as

$$\begin{aligned} a_k^\dagger &= \frac{1}{\sqrt{N}} \sum_{j=1}^N e^{-2ia_jk} a_j^\dagger, \\ b_k^\dagger &= \frac{1}{\sqrt{N}} \sum_{j=1}^N e^{2ia_jk} b_j^\dagger, \end{aligned} \quad (2.2)$$

where $k = \pi l / Na$ ($l = -N/2 + 1, -N/2 + 2, \dots, N/2$) with a being the distance between two neighboring spins. We note that here the unit cell is of length $2a$. Carrying out a Bogoliubov transformation

$$\begin{aligned} \alpha_k &= e^{-ia\lambda_k/2} \cosh\theta_k a_k + e^{ia\lambda_k/2} \sinh\theta_k b_k^\dagger, \\ \beta_k &= e^{ia\lambda_k/2} \sinh\theta_k a_k^\dagger + e^{-ia\lambda_k/2} \cosh\theta_k b_k, \end{aligned} \quad (2.3)$$

with

$$(1 + \delta)\tan[(k - \lambda_k)a] - (1 - \delta)\tan(ak) = 0, \quad (2.4)$$

$$\begin{aligned} \tan(2\theta_k) &= \frac{2\sqrt{Ss}}{(1 + \delta)(S + s)} \\ &\times \sqrt{(1 + \delta)^2 \cos^2(ak) + (1 - \delta)^2 \sin^2(ak)}, \end{aligned} \quad (2.5)$$

we reach the diagonal Hamiltonian,

$$\mathcal{H} = E_0 + \sum_k (\omega_k^- \alpha_k^\dagger \alpha_k + \omega_k^+ \beta_k^\dagger \beta_k), \quad (2.6)$$

where

$$\begin{aligned} E_0 &= -J(1 + \delta)SsNJ \\ &+ \frac{J}{2} \sum_k [\sqrt{(1 + \delta)^2(S-s)^2 + 16\delta Ss \sin^2(ak)} \\ &- (1 + \delta)(S + s)], \end{aligned} \quad (2.7)$$

$$\begin{aligned} \omega_k^\mp &= \frac{J}{2} [\sqrt{(1 + \delta)^2(S-s)^2 + 16\delta Ss \sin^2(ak)} \\ &\mp (1 + \delta)(S - s)]. \end{aligned} \quad (2.8)$$

Thus the spin-wave approach suggests the coexistence of the ferromagnetism and the antiferromagnetism in the present system. In the ferromagnetic branch (ω_k^-), the spin wave reduces the total magnetization and exhibits a quadratic dispersion relation in the small-momentum region:

$$\omega_{k \rightarrow 0}^- = \frac{J\delta Ss(2ak)^2}{(1 + \delta)(S - s)}, \quad (2.9)$$

while in the antiferromagnetic branch (ω_k^+), the spin wave enhances the total magnetization and have the gapped excitation spectrum:

$$\omega_{k \rightarrow 0}^+ = J(1 + \delta)(S - s) + \frac{J\delta Ss(2ak)^2}{(1 + \delta)(S - s)}. \quad (2.10)$$

As long as S and s are different from each other, the model keeps the two aspects of low-lying excitations. We further note that the qualitative character of the model remains unchanged over the whole region of δ . It is the purpose in this article to confirm this scenario employing efficient numerical methods.

III. A PERTURBATION APPROACH

Second, prior to the numerical approach, let us carry out a perturbation calculation with the intention of elucidating the nature of the elementary excitations. In the decoupled-dimer limit, we can easily find the low-lying eigenstates. Figures 1(a), 1(b), and 1(c) represent, respectively, the ground state, $|\Psi\rangle$, the ferromagnetic excitation at an arbitrary unit cell j , $|\Psi_j^\uparrow\rangle$, and the antiferromagnetic excitation at an arbitrary unit cell j , $|\Psi_j^\downarrow\rangle$, of the Hamiltonian (1.1) with $(S, s) = (1, 1/2)$ at $\delta=0$. When we turn on the exchange interaction between the dimers, the localized excitations can hop to neighboring unit cells with an amplitude proportional to δ . We take account of this effect using the degenerate perturbation. We introduce a representation of the matrix-product type as

$$|\Psi\rangle = g_1^{\uparrow s} \otimes h_1^s \otimes \cdots \otimes g_N^{\uparrow s} \otimes h_N^s, \quad (3.1)$$

$$|\Psi_j^\downarrow\rangle = g_1^{\uparrow s} \otimes h_1^s \otimes \cdots \otimes g_j^{\downarrow s} \otimes h_j^s \otimes \cdots \otimes g_N^{\uparrow s} \otimes h_N^s, \quad (3.2)$$

$$|\Psi_j^\uparrow\rangle = g_1^{\uparrow s} \otimes h_1^s \otimes \cdots \otimes g_j^{\uparrow +} \otimes h_j^+ \otimes \cdots \otimes g_N^{\uparrow s} \otimes h_N^s, \quad (3.3)$$

where

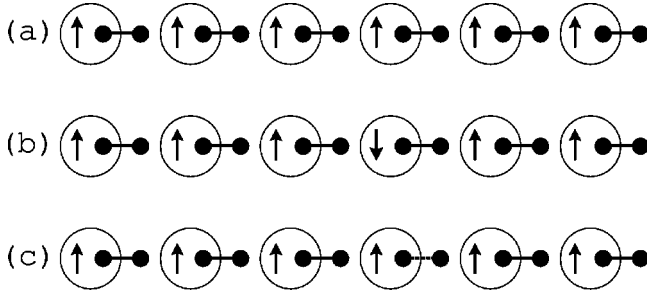


FIG. 1. Schematic representations of the ground state (a), the elementary excitation in the subspace of $M=N/2-1$ (b), and the elementary excitation in the subspace of $M=N/2+1$ (c) of the ferrimagnetic chain with spin 1 and spin 1/2 in the decoupled-dimer limit. The arrow (the bullet symbol) denotes a spin 1/2 with its fixed (unfixed) projection value. The solid (broken) segment is a singlet (triplet) pair. The circle represents an operation of constructing a spin 1 by symmetrizing the two spin 1/2's inside.

$$g_j^{\uparrow s} = [|0\rangle_j \sqrt{2}|+\rangle_j], \quad g_j^{\downarrow s} = [\sqrt{2}|-\rangle_j |0\rangle_j],$$

$$g_j^{\uparrow +} = [-\sqrt{2}|+\rangle_j |0\rangle], \quad (3.4)$$

$$h_j^s = \begin{bmatrix} -|\uparrow\rangle_j \\ |\downarrow\rangle_j \end{bmatrix}, \quad h_j^{\uparrow +} = \begin{bmatrix} -|\uparrow\rangle_j \\ 0 \end{bmatrix}, \quad (3.5)$$

with $|\pm\rangle_j$, $|0\rangle_j$ being the S_j^z eigenstates and $|\uparrow\rangle_j$, $|\downarrow\rangle_j$ the s_j^z eigenstates. Now the dispersion relations of the eigenstates with $M=N/2\mp 1$, ω_k^\mp , are calculated as

$$\omega_k^- = \frac{\langle \Psi_k^\downarrow | \mathcal{H} | \Psi_k^\downarrow \rangle}{\langle \Psi_k^\downarrow | \Psi_k^\downarrow \rangle} - E_G = \frac{4}{9} J \delta [1 - \cos(2ak)] + O(\delta^2), \quad (3.6)$$

$$\omega_k^+ = \frac{\langle \Psi_k^+ | \mathcal{H} | \Psi_k^+ \rangle}{\langle \Psi_k^+ | \Psi_k^+ \rangle} - E_G = \frac{3}{2} J + \frac{1}{18} J \delta [7 - 12 \cos(2ak)] + O(\delta^2), \quad (3.7)$$

where $|\Psi_k^\downarrow\rangle = N^{-1/2} \sum_{j=1}^N e^{-2iajk} |\Psi_j^\downarrow\rangle$ and $|\Psi_k^+\rangle = N^{-1/2} \sum_{j=1}^N e^{-2iajk} |\Psi_j^+\rangle$ are the Fourier transforms of $|\Psi_j^\downarrow\rangle$ and $|\Psi_j^+\rangle$, respectively, and $E_G = \langle \Psi | \mathcal{H} | \Psi \rangle / \langle \Psi | \Psi \rangle = -J(1 + \delta/9)N$ is the ground-state energy within the first order of δ . Although the Heisenberg point ($\delta=1$) is far from the decoupled-dimer limit, it is interesting enough that the qualitative characters of both branches remain unchanged as δ increases: The ferromagnetic branch ω_k^- is gapless and proportional to k^2 in the small- k region, while the antiferromagnetic branch ω_k^+ is gapped.

For an arbitrary combination of (S, s) , the similar argument can be developed and qualitatively the same result is obtained. For example, in the case of $(S, s) = (3/2, 1/2)$, we find the dispersion relations

$$\omega_k^- = \frac{5}{8} J \delta [1 - \cos(2ak)] + O(\delta^2), \quad (3.8)$$

$$\omega_k^+ = 2J + \frac{1}{8} J \delta [7 - 6 \cos(2ak)] + O(\delta^2), \quad (3.9)$$

with $E_G = -(5/4)J(1 + \delta/4)N$, considering the elementary excitations shown in Fig. 2. Thus we are more and more

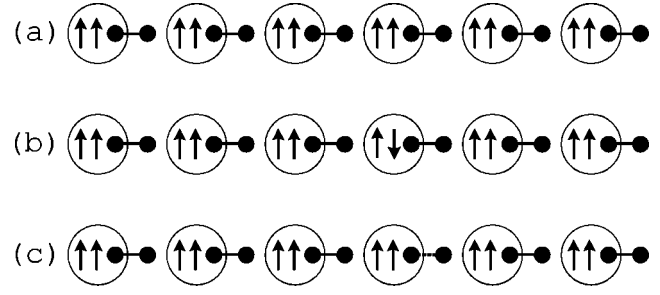


FIG. 2. Schematic representations of the ground state (a), the elementary excitation in the subspace of $M=N/2-1$ (b), and the elementary excitation in the subspace of $M=N/2+1$ (c) of the ferrimagnetic chain with spin 3/2 and spin 1/2 in the decoupled-dimer limit. The notation is the same as one in Fig. 1 except for the circle representing an operation of constructing a spin 3/2 by symmetrizing the three spin 1/2's inside.

convinced that the scenario of the low-energy structure should be valid for an arbitrary Heisenberg ferrimagnet. Actually, recent numerical studies^{22,24} on the present Hamiltonian reported that the low-temperature properties are essentially the same regardless of the values of S and s as long as they differ from each other. Alcaraz and Malvezzi²² found that the model with exchange anisotropy is described in terms of the Gaussian critical theory in both cases of $(S, s) = (1, 1/2)$ and $(S, s) = (3/2, 1/2)$. In such circumstances, we restrict our numerical investigation to the case of $(S, s) = (1, 1/2)$.

IV. NUMERICAL PROCEDURE

In order to calculate the low-lying eigenvalues of the model, we here use two numerical tools, which possess, respectively, both advantageous and weak points of their own and are complementary to each other. One is the exact-diagonalization method employing the Lanczos algorithm. Calculation of the energy levels reduces to the diagonalization of the $6^N \times 6^N$ matrix representing the Hamiltonian. In constructing basic states, we use direct products of the single-spin states indicated by the projection values. The present Hamiltonian commutes with the total magnetization M and therefore splits into $3N+1$ blocks labeled by M (on the assumption that N is even). Since we perform the calculation under the periodic boundary condition, each eigenvalue is further classified by its total wave number k .

We treat the chains of $N=8, 10, 12$, where we restrict the calculation to the lowest energy level in each subspace. Since our main interest is to reveal the nature of the elementary excitations, we investigate the subspaces of $M=N/2$ and $M=N/2\mp 1$ for all the chain lengths we treat. We calculate the subspaces of $M \leq N/2-2$ as well for $N=8, 10$ in order to further elucidate the ferromagnetic nature of the model. Due to the two kinds of spins, the construction of the basic states is somewhat complicated. The base dimension reaches ten million in the case of $N=12$ and $M=N/2-1$.

The chain length we can reach with the diagonalization method is much smaller than one with a Monte Carlo technique. However, having in mind the small correlation length of the present system,^{24,25} the diagonalization result is fruitful enough to obtain a general view of the low-energy struc-

ture. Actually, the ground-state energy for $N=12$ coincides with the $N \rightarrow \infty$ extrapolated value within the first five digits. We further note that even the ground-state energy for $N=8$ is so close to the thermodynamic-limit value as to show the coincidence within the first three digits. This fact is quite helpful in estimating the dispersion relations in the long-chain limit, although the eigenvalues for different chain lengths should be distinguished.

The other approach is based on a quantum Monte Carlo technique^{12,34–36} which one of the authors has recently developed. The idea is summarized as extracting the lower edge of the excitation spectrum from imaginary-time quantum Monte Carlo data at a low enough temperature. The imaginary-time correlation function $S(q, \tau)$ is generally defined as

$$S(q, \tau) = \langle e^{\mathcal{H}\tau} O_q^z e^{-\mathcal{H}\tau} O_{-q}^z \rangle, \quad (4.1)$$

where $O_q = N^{-1} \sum_{j=1}^N O_j e^{iqja_0}$ is the Fourier transform of an arbitrary local operator O_j with a_0 being the length of the unit cell, and $\langle A \rangle \equiv \text{Tr}[e^{-\beta\mathcal{H}} A] / \text{Tr}[e^{-\beta\mathcal{H}}]$ denotes the canonical average at a given temperature $\beta^{-1} = k_B T$. While $S(q, \tau)$ as a function of τ generally exhibits a complicated multiexponential decay, it may efficiently be evaluated at a sufficiently low temperature as³⁴

$$S(q, \tau) = \sum_l |\langle 1; k_0 | S_q^z | l; k_0 + q \rangle|^2 e^{-\tau[E_l(k_0 + q) - E_1(k_0)]}, \quad (4.2)$$

where $|l; k\rangle$ ($l=1, 2, \dots$) and $E_l(k)$ ($E_1(k) \leq E_2(k) \leq \dots$) are the l th eigenvector and eigenvalue of the Hamiltonian in the k -momentum space, and k_0 is the momentum at which the lowest-energy state in the subspace is located. Now it is reasonable to approximate $E_1(k_0 + q) - E_1(k_0)$ by the slope $-\partial \ln[S(q, \tau)] / \partial \tau$ in the large- τ region satisfying

$$\tau[E_2(k_0 + q) - E_1(k_0 + q)] \gg \ln \frac{|\langle 1; k_0 | S_q^z | n; k_0 + q \rangle|^2}{|\langle 1; k_0 | S_q^z | 1; k_0 + q \rangle|^2}, \quad (4.3)$$

for an arbitrary n .

In case the lower edge of the spectrum is separated from the upper bands or continuum by a finite gap, or in case of its spectral weights $|\langle 1; k_0 | O_q^z | 1; k_0 + q \rangle|^2$ being relatively large, the inequality (4.3) is well justified even at small τ 's and a logarithmic plot of $S(q, \tau)$ is expected to exhibit fine linearity in a wide region of τ . Actually, for single-spin Heisenberg chains with an arbitrary spin quantum number or a certain bond alternation, it was shown^{12,34–36} that the τ dependence of $S(q, \tau)$ is essentially approximated by a single exponent at each momentum q at a sufficiently low temperature.

Here, due to the two kinds of spins in a chain, O_j is not uniquely defined. We show in Fig. 3 logarithmic plots of $S(q, \tau)$ as a function of τ setting several operators for O_j . We have set $(\beta J)^{-1}$ and n equal to 0.02 and 200, which are, respectively, low and large enough³⁶ to remove the finite-temperature effect and the finite- n effect. In order to estimate each $S(q, \tau)$, we have carried out a few million Monte Carlo steps spending several days on a supercomputer or a few weeks on a fast workstation. Energy difference between the

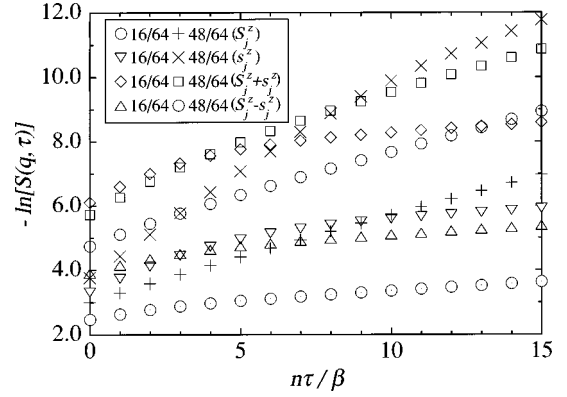


FIG. 3. Logarithmic plots of $S(q, \tau)$ versus the imaginary time τ at several choices of O_j taking a few values of momentum q for the Heisenberg ferrimagnetic chain of $N=32$ with $(S, s) = (1, 1/2)$ and $\delta=1$: \odot ($2aq/\pi=16/64$), \square ($2aq/\pi=48/64$) with $O_j=S_j^z$; ∇ ($2aq/\pi=16/64$), \times ($2aq/\pi=48/64$) with $O_j=S_j^z$; \diamond ($2aq/\pi=16/64$), \square ($2aq/\pi=48/64$) with $O_j=S_j^z + S_j^z$; \triangle ($2aq/\pi=16/64$), \square ($2aq/\pi=48/64$) with $O_j=S_j^z - S_j^z$. The numerical uncertainty is all within the size of the symbols.

ground state and the lowest state with an arbitrary q is obtained through $S(q, \tau)$ calculated in the subspace of $M=0$.

In Fig. 4 we plot the excitation energies as a function of q obtained by estimating the slope $-\partial \ln[S(q, \tau)] / \partial \tau$ in the largest- τ region available. In the case of $O_j=S_j^z$, the multiexponential behavior of $S(q, \tau)$ is remarkable even in the large- τ region and thus prevents us from precisely estimating the energy eigenvalues. In all the other cases, we obtain useful data within the numerical precision. With the present data, we can at least conclude that spin-1/2's do not have much effect on the lowest-lying excitations, which suggests that the elementary excitations of ferromagnetic nature may qualitatively be described by the simple picture shown in Fig. 1(b) even at the Heisenberg point $\delta=1$. While $O_j=S_j^z + S_j^z$ brings somewhat higher energies than $O_j=S_j^z$ and $O_j=S_j^z - S_j^z$, we find no difference beyond the numerical accuracy between the cases of $O_j=S_j^z$ and $O_j=S_j^z - S_j^z$. It will be

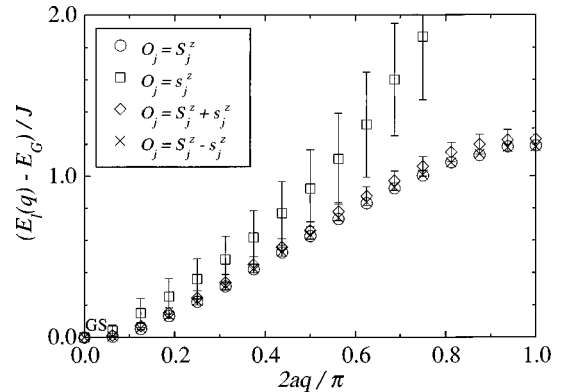


FIG. 4. Quantum Monte Carlo estimates of excitation energies as a function of q for the chain of $N=32$. Here \odot , \square , \diamond , and \times have, respectively, been obtained from $S(q, \tau)$'s with $O_j=S_j^z$, $O_j=S_j^z + S_j^z$, $O_j=S_j^z + S_j^z$, and $O_j=S_j^z - S_j^z$ at the subspace of $M=0$. The error bars are attached to the data obtained with $O_j=S_j^z$ and $O_j=S_j^z + S_j^z$. The numerical uncertainty of the rest of the data is all within the size of the symbols. GS denotes the ground state.

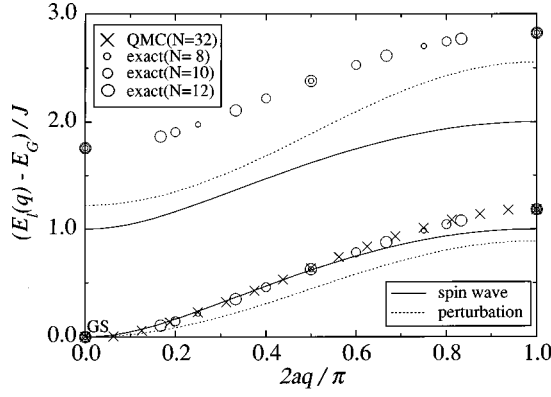


FIG. 5. Quantum Monte Carlo and exact-diagonalization calculations of the lowest energies as a function of momentum in the subspaces of $M = N/2 \mp 1$ for the Heisenberg ferrimagnetic chain of $N = 32$ with spin 1 and spin 1/2. The numerical uncertainty is all within the size of the symbols. The results of the spin-wave theory and the first-order perturbation from the decoupled-dimer limit are also shown by solid and broken lines, respectively. GS denotes the ground state.

shown in the next section that the thus-obtained lowest-lying energy eigenvalues are in good agreement with the exact-diagonalization result. This method is applicable to rather long chains but is not successful in obtaining the higher-lying eigenvalues except for the special fortunate cases.³⁴ Thus the diagonalization technique is necessary and useful for the antiferromagnetic branch with $M > N/2$ even though it is inferior to the Monte Carlo method in treating long chains.

V. NUMERICAL RESULTS AND DISCUSSION

We plot in Fig. 5 the quantum Monte Carlo and the exact-diagonalization calculations of the excitation energies as a function of momentum q for the chain without bond alternation, where the results of the spin-wave theory and the first-order perturbation from the decoupled-dimer limit are also shown. The lower band is the lower edge of the excitation spectrum and consists of the lowest-lying eigenvalues with $M = N/2 - 1$. It exhibits a quadratic dispersion at small q 's as was expected. The upper band consists of the lowest-lying eigenvalues with $M = N/2 + 1$ and is separated from the ground state by a finite gap. It is the scenario predicted by the analytic approaches that we here observe. The quantum Monte Carlo finding is in good agreement with the diagonalization result. The diagonalization calculation indicates that the chain-length dependence of the dispersion relation is quite weak even in the vicinity of the zone boundary and the zone center, which is consistent with the extremely small correlation length.^{24,25}

In order to perform a quantitative comparison between the numerical findings and the analytic results, let us consider the curvature of the dispersion, v , which is defined by

$$\omega_k^- = v(2ak)^2. \quad (5.1)$$

The quantum Monte Carlo method, the spin-wave calculation, and the perturbation approach, respectively, give $v^{\text{QMC}}/J = 0.37(1)$, $v^{\text{SW}}/J = 1/2$, and $v^{\text{pert}}/J = 2/9$. The spin-wave theory overestimates the true value, while the pertur-

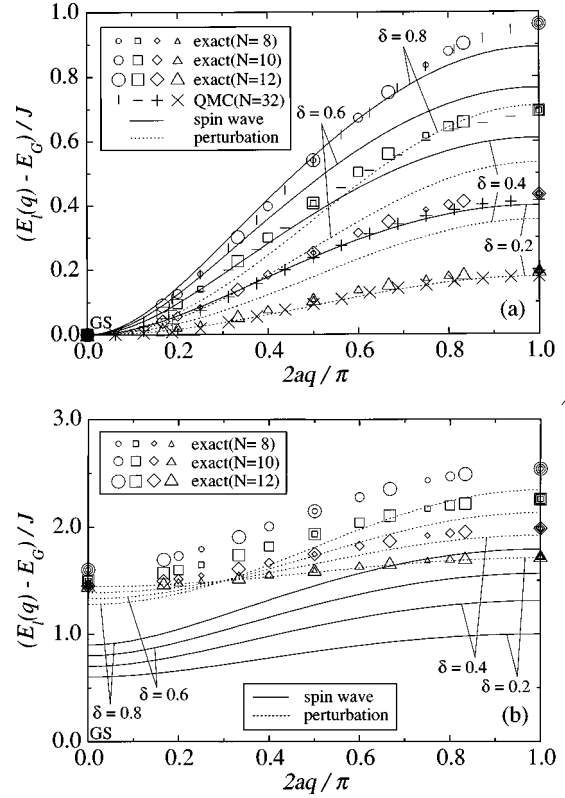


FIG. 6. The lowest energies as a function of momentum in the subspaces of $M = N/2 - 1$ (a) and $M = N/2 + 1$ (b) for the bond-alternating Heisenberg ferrimagnetic chains of $N = 32$ with spin 1 and spin 1/2. Here \circ (\square), \square ($-$), \diamond ($+$), and \triangle (\times) represent the exact-diagonalization (quantum Monte Carlo) estimates at $\delta = 0.8$, $\delta = 0.6$, $\delta = 0.4$, and $\delta = 0.2$, respectively. The numerical uncertainty is all within the size of the symbols. The results of the spin-wave theory and the first-order perturbation from the decoupled-dimer limit are also shown by solid and broken lines, respectively, where the values of δ are 0.8, 0.6, 0.4, and 0.2 from top to bottom except for the perturbation result for the antiferromagnetic branch in the small- q region with the values of δ being 0.2, 0.4, 0.6, and 0.8 from top to bottom. GS denotes the ground state.

bation approach underestimates that. We have made an attempt to obtain another estimate of v using the exact-diagonalization result. Although the Lanczos algorithm results in much more precise raw data than the Monte Carlo technique, yet the attempt was not as successful as one using the Monte Carlo data because of the lack of data points. However, we have confirmed that the diagonalization estimate of v possibly coincides with v^{QMC} within the numerical accuracy. We note that the spin-wave estimate v^{SW} accords with one for the Heisenberg ferromagnet of spin 1/2 in the unit of the unit-cell length being equal to unity. Furthermore the calculation of the lowest levels in the subspace of $M = N/2 - 2$ results in energy eigenvalues below the two-magnon continuum. The obtained state should be a two-magnon bound state.³⁷ All these facts again emphasize the ferromagnetic aspect of the present model. However, in contrast with the ferromagnet, the true value v^{QMC} is reduced from v^{SW} due to the quantum effect. Thus the elementary excitations in the sector of $M < N/2$ can be regarded as spin waves modified by quantum fluctuations.

For the antiferromagnetic branch, on the other hand, both

spin-wave analysis and perturbation calculation are not as successful as ones for the ferromagnetic branch. Considering that quantum effects are, in general, much more remarkable in antiferromagnets than in ferromagnets, the most naive picture of the elementary excitations illustrated in Figs. 1 and 2 may have to be significantly modified for the antiferromagnetic branch.

Finally in this section, we show in Fig. 6 the calculation for the chains with bond alternation. Although the quantum Monte Carlo calculation is generally in good agreement with the diagonalization result, the agreement seems to be somewhat poorer in the small- δ region. This is convincing keeping in mind that the decrease of δ may cause the freezing of the spin configuration in Monte Carlo sampling and therefore a huge number of Monte Carlo steps are needed to refine the data accuracy in the small- δ region. It is needless to say that the perturbation calculation is more justified in the small- δ region. As the model approaches the decoupled-dimer limit, both ferromagnetic and antiferromagnetic bands become flatter and approach 0 and $(3/2)J$, respectively. The spin-wave result is fairly good in the ferromagnetic branch but relatively poor in the antiferromagnetic branch. This is convincing considering that the spin wave correctly describes the low-lying excitations of the ferromagnets, while it is valid at most qualitatively for the antiferromagnets.

VI. SUMMARY

We have investigated the low-energy structure of the ferrimagnetic alternating-spin chains with spin 1 and spin 1/2. Motivated by the spin-wave analysis of the model, we have mainly calculated the eigenvalues with an arbitrary momentum of the one-magnon states, namely, the lowest-lying eigenvalues in the subspaces of $M = N/2 \mp 1$. The chain-length dependence of the dispersion relations is extremely weak, which is consistent with the considerably small correlation length of the system, $\xi < 2a$.^{24,25} The qualitative character of the model remains unchanged under the existence of bond

alternation. The ferromagnetic branch is gapless and shows a quadratic dispersion in the small-momentum region, while the antiferromagnetic branch is separated from the ground state by a finite gap Δ . Δ/J in the thermodynamic limit is estimated to be 1.759 14(1) at the Heisenberg point $\delta=1$. We made an attempt to understand the low-lying excitations through the first-order perturbation calculation from the decoupled-dimer limit. The ferromagnetic excitations are more or less dominated by spin 1's, whereas the mechanism of the antiferromagnetic excitations was less revealed. Quantum Monte Carlo snapshots³⁸ may help us to inquire further into the antiferromagnetic fluctuations.

We have further carried out the diagonalization calculation in the subspace of $M = N/2 - 2$ and found the two-magnon bound state below the continuum. This fact emphasizes the ferromagnetic aspect of the sector of $M < N/2$ in the ferrimagnet. We expect that the Heisenberg ferrimagnet behaves like a ferromagnet at low enough temperatures, while its antiferromagnetic aspect may appear at $k_B T \gtrsim \Delta$.

ACKNOWLEDGMENTS

A part of this work was carried out while S.Y. was staying at the Hannover Institute for Theoretical Physics. S.Y. gratefully acknowledges the hospitality of the institute at that time. The authors would like to thank U. Neugebauer for his great help in coding the Lanczos algorithm. They are further grateful to T. Tonegawa, T. Fukui, and S. K. Pati for their useful comments. This work was supported by the German Federal Ministry for Research and Technology (BMBF) under Contract No. 03-MI4HAN-8, by the Japanese Ministry of Education, Science, and Culture through Grant-in-Aid No. 09740286, and by a Grant-in-Aid from the Okayama Foundation for Science and Technology. Most of the numerical computation was done using the facility of the Zuse Computing Center, Berlin and the Supercomputer Center, Institute for Solid State Physics, University of Tokyo.

¹F. D. M. Haldane, Phys. Lett. **93A**, 464 (1983); Phys. Rev. Lett. **50**, 1153 (1983).

²S. R. White and D. A. Huse, Phys. Rev. B **48**, 3844 (1993).

³E. S. Sørensen and I. Affleck, Phys. Rev. Lett. **71**, 1633 (1993).

⁴O. Golinelli, Th. Jolicœur, and R. Lacaze, Phys. Rev. B **50**, 3037 (1994).

⁵U. Schollwöck and Th. Jolicœur, Europhys. Lett. **30**, 493 (1995).

⁶S. Yamamoto, Phys. Lett. A **213**, 102 (1996).

⁷I. Affleck, T. Kennedy, E. H. Lieb, and H. Tasaki, Phys. Rev. Lett. **59**, 799 (1987); Commun. Math. Phys. **115**, 477 (1988).

⁸I. Affleck, Nucl. Phys. B **257**, 397 (1985); **265**, 409 (1986).

⁹R. R. P. Singh and M. P. Gelfand, Phys. Rev. Lett. **61**, 2133 (1988).

¹⁰Y. Kato and A. Tanaka, J. Phys. Soc. Jpn. **63**, 1277 (1994).

¹¹S. Yamamoto, J. Phys. Soc. Jpn. **63**, 4327 (1994); Phys. Rev. B **52**, 10 170 (1995).

¹²S. Yamamoto, Phys. Rev. B **51**, 16 128 (1995).

¹³K. Totsuka and M. Suzuki, J. Phys.: Condens. Matter **7**, 1639 (1995).

¹⁴M. Yajima and M. Takahashi, J. Phys. Soc. Jpn. **65**, 39 (1996).

¹⁵S. Yamamoto, Phys. Rev. B **55**, 3603 (1997).

¹⁶M. Oshikawa, M. Yamanaka, and I. Affleck, Phys. Rev. Lett. **78**, 1984 (1997).

¹⁷K. Totsuka, Phys. Lett. A **228**, 103 (1997).

¹⁸S. R. Aladim and M. J. Martins, J. Phys. A **26**, L529 (1993); M. J. Martins, *ibid.* **26**, 7301 (1993).

¹⁹H. J. de Vega and F. Woynarovich, J. Phys. A **25**, 4499 (1992); H. J. de Vega, L. Mezincescu, and R. I. Nepomechie, Phys. Rev. B **49**, 13 223 (1994).

²⁰P. Schlottmann, Phys. Rev. B **49**, 9202 (1994).

²¹M. Fujii, S. Fujimoto, and N. Kawakami, J. Phys. Soc. Jpn. **65**, 2381 (1996).

²²F. C. Alcaraz and A. L. Malvezzi, J. Phys. A **30**, 767 (1997).

²³A. K. Kolezhuk, H.-J. Mikeska, and S. Yamamoto, Phys. Rev. B **55**, 3336 (1997).

²⁴S. K. Pati, S. Ramasesha, and D. Sen, Phys. Rev. B **55**, 8894 (1997); J. Phys.: Condens. Matter **9**, 8707 (1997).

²⁵S. Brehmer, H.-J. Mikeska, and S. Yamamoto, J. Phys.: Condens. Matter **9**, 3921 (1997).

- ²⁶T. Fukui and N. Kawakami, Phys. Rev. B **55**, 14 709 (1997); **56**, 8799 (1997).
- ²⁷H. Niggemann, G. Uimin, and J. Zittartz, J. Phys.: Condens. Matter **9**, 9031 (1997).
- ²⁸T. Ono, T. Nishimura, M. Katsumura, T. Morita, and M. Sugimoto, J. Phys. Soc. Jpn. **66**, 2576 (1997).
- ²⁹T. Tonegawa, T. Hikihara, T. Nishino, M. Kaburagi, S. Miyashita, and H.-J. Mikeska, J. Magn. Magn. Mater. (to be published).
- ³⁰T. Kuramoto, cond-mat/9710229 (unpublished).
- ³¹O. Kahn, Y. Pei, and Y. Journaux, in *Inorganic Materials*, edited by D. W. Bruce and D. O'Hare (Wiley, New York, 1992), p. 95.
- ³²E. Lieb and D. Mattis, J. Math. Phys. **3**, 749 (1962).
- ³³J. Goldstone, A. Salam, and S. Weinberg, Phys. Rev. **127**, 965 (1962).
- ³⁴S. Yamamoto and S. Miyashita, J. Phys. Soc. Jpn. **63**, 2866 (1994); Phys. Lett. A **235**, 545 (1997).
- ³⁵S. Yamamoto, Phys. Rev. Lett. **75**, 3348 (1995).
- ³⁶S. Yamamoto, Int. J. Mod. Phys. C **8**, 609 (1997).
- ³⁷D. C. Mattis, *The Theory of Magnetism I* (Springer-Verlag, Berlin, 1988), p. 155.
- ³⁸S. Yamamoto and S. Miyashita, Phys. Rev. B **48**, 9528 (1993).